Hybrid Chemical Vapor Deposition/Sol−Gel Route in the Preparation of Nanophasic $LaCoO_3$ Films

Lidia Armelao, Davide Barreca,* and Gregorio Bottaro

ISTM-CNR and INSTM, Department of Chemistry, Padova University, Via Marzolo 1, 35131 Padova, Italy

Alberto Gasparotto, Cinzia Maragno, and Eugenio Tondello

INSTM, Department of Chemistry, Padova University, Via Marzolo 1, 35131 Padova, Italy

Received June 29, 2004. Revised Manuscript Received November 2, 2004

Lanthanum cobaltite ($LaCoO_3$) thin films were synthesized by an innovative route based on the combination of chemical vapor deposition (CVD) and sol−gel (SG) methods. In particular, the approach is based on the sequential deposition of binary oxide systems (Co−O on La−O) and on the ex situ thermal treatment of the final product (T = 400−900 °C, t = 1−8 h), aimed at favoring solid-state reactions for the formation of a ternary La−Co−O nanosystem. To highlight the peculiar effects of these procedures on the characteristics of the final product, both SG and CVD routes were used for the preparation of single-phase La−O and Co−O species. The process resulted in the formation of $LaCoO_3$ nanostructured films with an average crystallite size lower than 20 nm. The required processing conditions were strongly dependent on the specific synthetic pathway: (i) SG of Co−O on CVD La−O; (ii) CVD of Co−O on SG La−O. In this framework, particular attention was focused on the analogies and differences between the two sequences and on a study of the most relevant compositional, structural, and morphological system features.

Introduction

Among the $LaMO_3$ (M = Co, Mn, Cu, Fe) perovskite-type oxides, lanthanum cobaltite ($LaCoO_3$) is extremely promising for different technological applications, owing to its physical and chemical properties.[1,2] In particular, $LaCoO_3$ systems show a remarkable activity for NO_x decomposition and oxidation of CO and hydrocarbons,[3−7] which has justified their use in environmental catalysis[8,9] and in the conversion of exhaust gases into nontoxic products.[3,7,8] Moreover, lanthanum cobaltite has been used in sensors for reducing gases (such as CO, CH_3OH, and CH_3CH_2OH[1,10,11]) and in solid oxide fuel cells (SOFCs), both as cathodes, thanks to their thermal stability and oxygen deficiencies,[12] and as solid electrolytes, due to their oxygen permeability.[13,14] The major drawback in these applications concerns the necessity for high working temperatures (>600 °C), to overcome kinetic limitations and attain a sufficient ionic conductivity.[2] The consequent device degradation, due to both thermal effects and parasitic electrolyte−electrode reactions, has stimulated several research efforts aimed at reducing the operational temperatures.

In this context, one of the most appealing alternatives is offered by the synthesis of $LaCoO_3$ nanosystems, whose use might be, in principle, very advantageous thanks to the synergy between oxygen deficiencies and their high surface-to-volume ratio. Since the activity of such materials is strongly dependent on the synthetic procedure,[15−17] more and more attention is being devoted to the development of suitable strategies to obtain nanosystems with tailored composition and structure. Until now, nanophasic lanthanum cobaltite has been mainly obtained in the form of powders,[6,8,11,16−18] and only a few papers concerning the preparation of nanophasic $LaCoO_3$ thin films are available in the literature.[3,4,9,19−22]

* To whom correspondence should be addressed. E-mail: davide@chin.unipd.it. Phone: +39-0498275170. Fax: +39-0498275161.

(1) Peña, M. A.; Fierro, J. L. G. *Chem. Rev.* **2001**, *101*, 1981.
(2) Boudghene Stambouli, A.; Traversa, E. *Renewable Sustainable Energy Rev.* **2002**, *6*, 433.
(3) Hwang, H. J.; Awano, M. *J. Eur. Ceram. Soc.* **2001**, *21*, 2103.
(4) Hwang, H. J.; Moon, J.; Awano, M.; Maeda, K. *J. Am. Ceram. Soc.* **2000**, *83*, 2852.
(5) Nguyen, S. V.; Szabo, V.; Trong On, D.; Kaliaguine, S. *Microporous Mesoporous Mater.* **2002**, *54*, 51.
(6) Simonot, L.; Garin, F.; Maire, G. *Appl. Catal., B* **1997**, *11*, 167.
(7) Simonot, L.; Garin, F.; Maire, G. *Appl. Catal., B* **1997**, *11*, 181.
(8) Singh, R. N.; Lal, B. *Int. J. Hydrogen Energy* **2002**, *27*, 45.
(9) Hwang, H. J.; Towata, A.; Awano, M.; Maeda, K. *Scr. Mater.* **2001**, *44*, 2173.
(10) Seim, H.; Nieminen, M.; Niinistö, L.; Fjellvåg, H.; Johansson, L.-S. *Appl. Surf. Sci.* **1997**, *112*, 243.
(11) Orlovskaya, N.; Kleveland, K.; Grande, T.; Einarsrud, M. A. *J. Eur. Ceram. Soc.* **2000**, *20*, 51.
(12) Minh, N. Q.; Takahashi, T. *Science and Technology of Ceramic Fuel Cells*; Elsevier: Amsterdam, The Netherlands, 1995.
(13) Chen, C. H.; Bouwmeester, H. J. M.; van Doorn, R. H. E.; Kruidhof, H.; Burggraaf, A. J. *Solid State Ionics* **1997**, *98*, 7.
(14) Balachandran, U.; Dusek, J. T.; Mieville, R. L.; Poeppel, R. P.; Kleefish, M. S.; Pei, S.; Kobylinski, T. P.; Udovich, C. A.; Bose, A. C. *Appl. Catal., A* **1995**, *133*, 19.
(15) Schwaz, J. A.; Contescu, C.; Contescu, A. *Chem. Rev.* **1995**, *95*, 477.
(16) Xiong, G.; Zhi, Z. L.; Yang, X.; Lu, L.; Wang, X. *J. Mater. Sci. Lett.* **1997**, *16*, 1064.
(17) Hackenberger, M.; Stephan, K.; Kiebling, D.; Schmitz, W.; Wendt, G. *Solid State Ionics* **1997**, *101−103*, 1195.
(18) Armelao, L.; Bandoli, G.; Barreca, D.; Bettinelli, M.; Bottaro, G.; Caneschi, A. *Surf. Interface Anal.* **2002**, *34*, 112.
(19) Bontempi, E.; Armelao, L.; Barreca, D.; Bertolo, L.; Bottaro, G.; Pierangelo, E.; Depero, L. E. *Cryst. Eng.* **2002**, *5*, 291.
(20) Shimizu, Y.; Murata, T. *J. Am. Ceram. Soc.* **1997**, *80*, 2702.
(21) Hattori, T.; Matsui, T.; Tsuda, H.; Mabuchi, H.; Morii, K. *Thin Solid Films* **2001**, *388*, 183.

10.1021/cm0489643 CCC: $30.25
Published on Web 12/29/2004

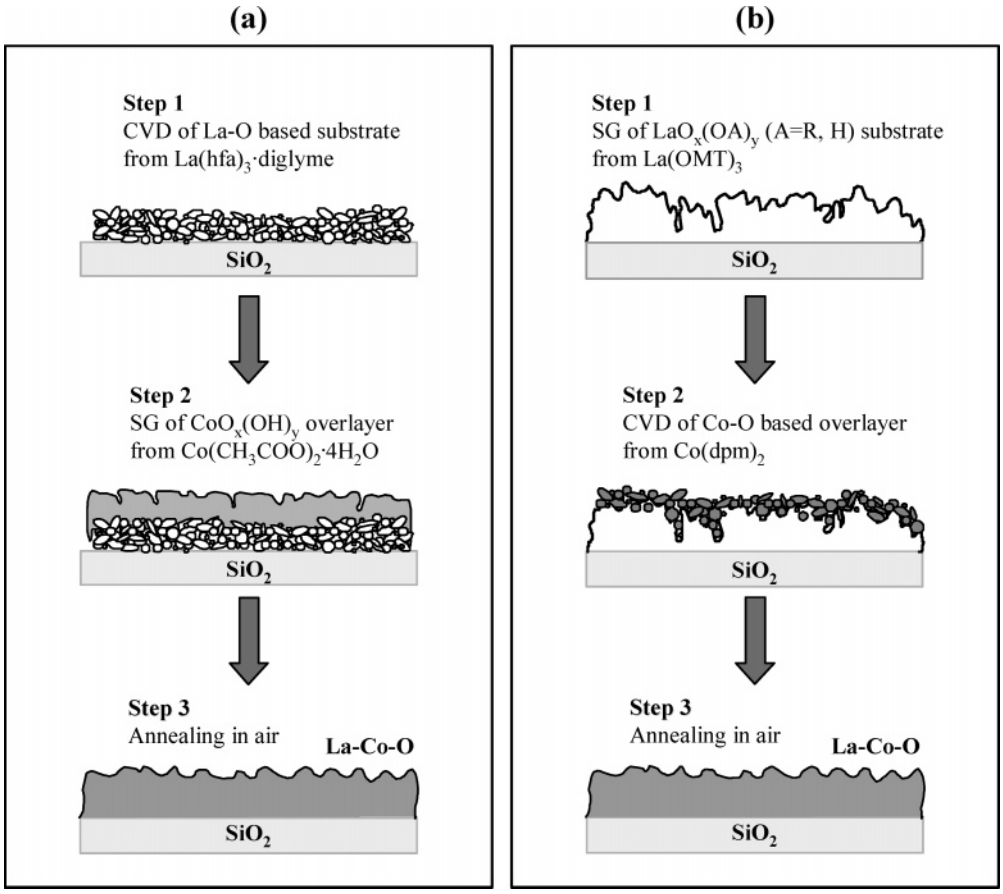

Figure 1. Schematic representation of the hybrid CVD/SG routes adopted for the preparation of $LaCoO_3$ nanosystems.

On the basis of our recent work on innovative chemical vapor deposition (CVD)/sol−gel (SG) routes to metal oxide nanosystems,[23,24] the present study is focused on a synthetic approach to nanostructured $LaCoO_3$ films (Figure 1). To the best of our knowledge, similar *hybrid* CVD/SG routes to $LaCoO_3$ nanosystems have not been reported so far. The proposed route is based on three successive steps: (1) deposition of La−O specimens; (2) covering with a Co−O overlayer; (3) annealing in air. In particular, both CVD and SG routes were used to prepare La−O and Co−O systems. In the former case (Figure 1a), CVD La−O systems deposited at low temperatures were used as substrates. Compared with conventional supports, these films offer, in principle, a higher contact area with the starting SG solution, thus enabling a sort of *percolation* of the SG layer into the CVD one.

When the as-prepared SG La−O systems ($LaO_x(OA)_y$ xerogels, where A = R, H) are used as substrates (Figure 1b), their porous structure, which is endowed with *nonbridging* groups (−OH and −OR), can provide reaction sites for successive chemical modifications on both the surface and subsurface layers.[23,24] Moreover, the CVD infiltration power further promotes the nucleation into the porous structure, resulting in an intimate intermixing between the two layers already during the deposition process.[23,24] In both cases reported in Figure 1, such intermixing phenomena are expected to favor the subsequent thermally induced La−Co−O reactions, ultimately leading to the formation of $LaCoO_3$. On the basis of these results, the use of a *combined* CVD/SG approach might be more advantageous with respect to a simple CVD (or SG) process.

In the end, the obtained systems were annealed in air, with the aim of investigating the formation of nanocrystalline $LaCoO_3$ as a function of the synthesis and processing conditions.

The evolution of the system under annealing was investigated in detail by means of a multitechnique characterization. The structural properties were analyzed by glancing incidence X-ray diffraction (GIXRD), while the surface and in-depth chemical compositions were studied by X-ray photoelectron spectroscopy (XPS) and X-ray-excited Auger electron spectroscopy (XE-AES). Finally, the surface topography was examined by atomic force microscopy (AFM).

Experimental Section

Synthesis. As shown in Figure 1, the syntheses reported in this work may be classified into two different categories, depending on the technique adopted for the preparation of the La−O substrates. In both cases, the production of single-phase $LaCoO_3$ nanosystems required the optimization of La/Co relative amounts as well as of the annealing conditions.

In the first part of the work (Figure 1a), La−O-based films were synthesized on silica slides (Herasil, Heraeus) by CVD at 200 °C

(22) Zhang, Y.; Zhu, Y.; Ye, X.; Cao, L. *Surf. Interface Anal.* **2001**, *32*, 310.
(23) Armelao, L.; Barreca, D.; Bottaro, G.; Gasparotto, A.; Tondello, E.; Ferroni, M.; Polizzi, S. *Chem. Vap. Deposition*, **2004**, *10*, 257.
(24) Armelao, L.; Barreca, D.; Bigliani, L.; Bottaro, G.; Gasparotto, A.; Tondello, E. *Electrochem. Soc. Proc.* **2003**, *8*, 1119.

using $La(hfa)_3$·diglyme (Hhfa = 1,1,1,5,5,5-hexafluoro-2,4-pentanedione; diglyme = bis(2-methoxyethyl) ether)[25] as precursor. Before the depositions, the substrates were cleaned according to the following procedure:[26] (i) washing with liquid soap diluted in deionized water, (ii) rinsing with deionized water to eliminate eventual detergent residuals, (iii) dipping in acetone, (iv) dipping in 2-propanol, and (v) air-drying. The compound was synthesized according to a literature procedure[25] and vaporized at 110 °C in each CVD experiment (duration 50 min). While nitrogen was used as carrier gas, an O_2 flow was introduced separately into the reaction chamber after it was passed through a water reservoir kept at 50 °C. Experiments were carried out under optimized pressure/gas flow conditions (total pressure 10 mbar, $\Phi(N_2) = 50$ sccm, $\Phi(O_2 + H_2O) = 100$ sccm). The cobalt oxide-based overlayers were prepared by SG dip-coating starting from a methanolic solution of $Co(CH_3COO)_2 \cdot 4H_2O$[27] (Acros Organics, 97%; $c(CoO) \approx 26$ g/L) by means of three successive dippings at a constant withdrawal speed (7 cm/min).

In the second part of the work (Figure 1b), lanthanum oxide xerogels were prepared on previously cleaned silica slides (see above) by SG dip-coating from ethanolic solutions of $La(OMT)_3$ (−OMT = 2-methoxyethoxy) (Aldrich, 10−12 wt % solution in 2-methoxyethanol; $c(La_2O_3) \approx 25$ g/L) at a withdrawal speed of 50 cm/min. Co−O-based films were synthesized by CVD using $Co(dpm)_2$ (Hdpm = 2,2,6,6-tetramethyl-3,5-heptanedione) as cobalt source.[28] The precursor was vaporized at 90 °C and carried onto the substrate surface ($T = 300$ °C) in an O_2 flow (total pressure 10 mbar, $\Phi(O_2) = 150$ sccm, duration 30 min).

In both cases, the processing conditions were chosen after preliminary experiments aimed at obtaining a La/Co atomic ratio close to the stoichiometric one in the final system.

The as-prepared samples were subsequently annealed in air between 400 and 900 °C for 1−8 h, to promote La−O/Co−O intermixing and reaction processes, inducing the formation of $LaCoO_3$.

Characterization. GIXRD patterns were recorded using a Bruker D8 Advance instrument equipped with a Göbel mirror and a Cu Kα source (40 kV, 40 mA), at incidence angles varying between 0.5° and 1.5°. The average crystallite dimensions were estimated by means of the Scherrer equation. In the case of $LaCoO_3$, the estimation was performed on the peak at $2\vartheta = 47.5°$, since the most intense signal at $2\vartheta = 33.4°$ arises from multiple reflections (see the Results and Discussion).

XPS and XE-AES analyses were run on a Perkin-Elmer Φ 5600ci spectrometer with a monochromatized Al Kα (1486.6 eV) source, at a working pressure lower than 10^{-9} mbar. The spectrometer was calibrated by assigning to the $Au4f_{7/2}$ line a binding energy (BE) of 84.0 eV with respect to the Fermi level. Charge neutralization with a low-energy flood gun was adopted. The residual BE shifts were corrected by assigning to the C1s line of adventitious carbon a value of 284.8 eV.[29] The estimated standard deviation for the BEs was ±0.2 eV. Detailed spectra were recorded in the following regions: Co2p, CoLMM, La3d, O1s, C1s, F1s. After a Shirley-type background subtraction,[30] the raw photoelectron peaks were fitted using a nonlinear least-squares deconvolution program adopting Gaussian−Lorentzian shapes. The atomic compositions were evaluated using sensitivity factors provided by Φ V5.4A software. Depth profiles were carried out by Ar^+ sputtering at 3.0 kV, with an argon partial pressure of 5×10^{-8} mbar. The sample thickness was evaluated by measuring the erosion crater depth at the end of each profile by means of a Tencor Alpha Step profiler.

AFM analyses were carried out using a Park Autoprobe CP instrument operating in contact mode and in air. The background was subtracted from the images using the ProScan 1.3 software from Park Scientific. Images were recorded in different sample areas to check the surface homogeneity.

Results and Discussion

The optimal synthesis conditions for the formation of pure and nanophasic $LaCoO_3$ thin films were adjusted through repeated preliminary experiments, which also ensured the reproducibility of the sample characteristics.

In the first part of this work (Figure 1a), La−O-based films were deposited onto silica by CVD and used as substrates for the SG deposition of cobalt oxides. To benefit from the method advantages, La−O depositions were performed at temperatures as low as 200 °C (see the Experimental Section), to ensure the formation of a not fully densified structure that would favor the successive conversion into the ternary La−Co−O phase. The La−O-based systems obtained under the above conditions were characterized by the absence of GIXRD peaks. Compositional analyses by XPS revealed the presence of La (10 atom %), C (36 atom %), F (22 atom %), and O (32 atom %). The La3d photopeak presented a satellite structure,[31] with the $j = 5/2$ components centered at BE = 835.9 and 838.3 eV. The F1s signal was fitted by two different components. The most intense, at BE = 688.1 eV, was assigned to F-containing hydrocarbon residuals,[32] thus suggesting an incomplete $La(hfa)_3$·diglyme decomposition under the adopted conditions. This finding was corroborated by the multicomponent structure of the C1s signal, which was detected even in the inner sample layers. The second F1s component was located at BE = 685.0 eV and ascribed to lattice fluorine in lanthanum oxyfluoride.[33] The incorporation of precursor residuals in the layer might be partially responsible for the system structural disorder, as proved by GIXRD. The O1s signal resulted from the contribution of two bands at BE = 529.8 and 532.0 eV, attributed to lanthanum oxyfluoride[33] and to hydroxyl/carbonate species, respectively.[32,34] While −OH species might be due to water presence during CVD depositions, carbonate formation could arise from interactions with the outer atmosphere.[34] Different attempts to eliminate fluorine contaminations by varying either H_2O vaporization (from room temperature to 90 °C) or the substrate temperature (200−500 °C) did not lead to F-free lanthanum oxide systems. This finding is in agreement with the results

(25) Malandrino, G.; Licata, R.; Castelli, F.; Fragalà, I. L.; Benelli, C. *Inorg. Chem.* **1995**, *34*, 6233.
(26) Armelao, L.; Bertoncello, R.; Coronaro, S.; Glisenti, A. *Sci. Technol. Cult. Heritage* **1998**, *7*, 41.
(27) Armelao, L.; Barreca, D.; Gross, S.; Martucci, A.; Tieto, M.; Tondello, E. *J. Non-Cryst. Solids* **2001**, *293*−*295*, 477.
(28) Barreca, D.; Massignan, C.; Daolio, S.; Fabrizio, M.; Piccirillo, C.; Armelao, L.; Tondello, E. *Chem. Mater.* **2001**, *13*, 588.
(29) Briggs, D.; Seah, M. P. *Practical Surface Analysis*, 2nd ed.; J. Wiley & Sons: New York, 1990.
(30) Shirley, D. A. *Phys. Rev.* **1972**, *55*, 4709.
(31) Vasquez, R. P. *Phys. Rev. B* **1996**, *54*, 14938.
(32) Moulder, J. F.; Stickle, W. F.; Sobol, P. W.; Bomben, K. D. *Handbook of X-ray Photoelectron Spectroscopy*; Perkin-Elmer: Eden Prairie, MN, 1992.
(33) Ryzhkov, M. V.; Gubanov, V. A.; Butzman, M. P.; Hagström, A. L.; Kurmaev, E. Z. *J. Electron Spectrosc. Relat. Phenom.* **1980**, *21*, 193.
(34) Burroughs, P.; Hamnett, A.; Orchard, A. F.; Thornton, G. *J. Chem. Soc., Dalton Trans.* **1976**, *17*, 1686.

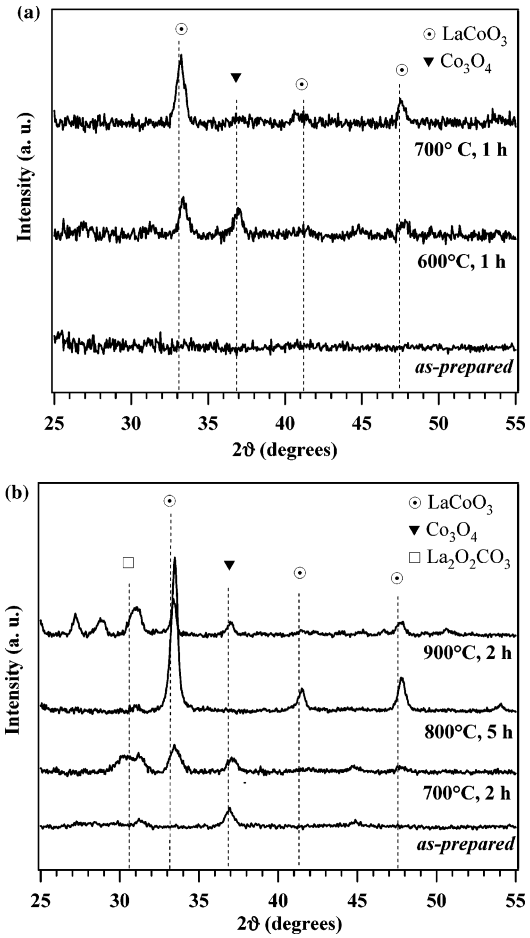

Figure 2. Representative GIXRD patterns as a function of annealing conditions for La−Co−O specimens obtained by **(a)** SG deposition of cobalt oxides on CVD La−O systems and **(b)** CVD of cobalt oxides on $LaO_x(OA)_y$ xerogels. The reflections reported from bulk $LaCoO_3$,[36,37] Co_3O_4,[38] and $La_2O_2CO_3$ [40] are evidenced.

obtained in the CVD of rare earth oxides from precursors similar to the lanthanum one adopted in this work.[35]

The obtained systems were subsequently used as substrates for the SG preparation of cobalt oxides under different conditions, to tailor the relative La/Co amount. These depositions were followed by annealing in air, aimed at checking the possibility of obtaining nanophasic $LaCoO_3$. Thermal treatments were carried out at different temperatures, and selected GIXRD patterns are displayed in Figure 2a. In this case, the as-prepared specimen did not present any diffraction peak. The appearance of $LaCoO_3$ reflections required thermal treatments at temperatures as high as 600 °C. However, the severe overlap of reflections from lanthanum cobaltite cubic (c)[36] and rhombohedral (r)[37] polymorphs prevented an unambiguous phase identification. In particular, the signal at $2\vartheta = 33.4°$ could be ascribed to $(110)_r$, $(104)_r$, and $(110)_c$ planes, while the peak at $2\vartheta = 47.7°$ was due to $(024)_r$ and $(200)_c$ ones. Finally, the signal at $2\vartheta = 37.0°$ was attributed to the (311) planes of fcc Co_3O_4.[38] More severe thermal treatments (700 °C, 1 h) induced the disappearance of Co_3O_4 reflections, and the weak peak at $2\vartheta = 41.5°$ $[(006)_r, (202)_r, (111)_c]$ further confirmed the complete formation of $LaCoO_3$. The average nanocrystal size was ≈18 nm. Moreover, no reflections from F-containing phases and/or La−O and Co−O ones were observed. Annealing at 800 °C for 1 h resulted in lanthanum cobaltite decomposition, as indicated by the absence of the corresponding diffraction peaks.[19,22]

A further aspect which concerns the specimens obtained by depositing cobalt oxides via CVD on $LaO_x(OA)_y$ xerogels (A = R, H) should be taken into account. To exploit the advantages of the combined CVD/SG route, the xerogel modifications during CVD experiments should be minimized by the use of mild conditions. In fact, high growth temperatures might induce a remarkable decrease of the amounts of nonbridging bonds (−OH) and a loss of the xerogel porous structure.[39] A temperature of 300 °C was proved to be the lowest possible for a uniform Co−O coverage of SG layers. This value was lower than that required for CVD experiments on conventional glass substrates[28] and thus confirms the *active role* of xerogel substrates during CVD deposition. Such behavior was ascribed to the presence of −OH groups in the SG matrix, acting as nucleation sites and enhancing the $Co(dpm)_2$ conversion into Co−O species. In this regard it is worth noting that no vapor phase decomposition of this complex was ever observed under the adopted operational conditions.[28]

The microstructural evolution observed under annealing (Figure 2b) proved to be notably different from that of the previous case. The as-prepared specimen presented reflections at $2\vartheta = 31.5°$, 37.0°, and 45.2°, ascribed to the (220), (311), and (400) planes, respectively, of fcc Co_3O_4[38] (crystallite size ≈15 nm). These characteristics showed almost no changes when the annealing temperature was increased to 500 °C. For $T \geq 600$ °C, weak and broadened signals in the $25° < 2\vartheta < 32°$ and $42° < 2\vartheta < 46°$ regions were observed and ascribed to xerogel crystallization in the form of lanthanum oxycarbonates. Annealing at 700 °C for 2 h resulted in the appearance of $LaCoO_3$ reflections at $2\vartheta = 33.4°$ and 47.8°. In the same spectrum, the broad peak at $2\vartheta \approx 30°$ could be attributed to the presence of lanthanum oxycarbonate ($La_2O_2CO_3$).[40] The absence of lanthanum oxide reflections was related to the ability of lanthanum oxide species to adsorb water and CO_2.[34]

An increase in the treatment temperature to 800 °C led to a gradual increase in the $LaCoO_3$ signal intensity, whereas reflections from other phases completely disappeared after a prolonged annealing (5 h, Figure 2b). Such behavior indicated that under the adopted conditions the only formed crystalline phase was $LaCoO_3$, with a typical crystallite size of ≈15 nm. It is worth observing that, when SG cobalt oxides were deposited onto CVD La−O substrates, the annealing temperature required for $LaCoO_3$ formation was lower (700 °C; compare Figure 2a). This difference could be attributed to the different evolutions of the system in the two cases,

(35) Lo Nigro, R.; Toro, R.; Malandrino, G.; Raineri, V.; Fragalà, I. L. *Electrochem. Soc. Proc.* **2003**, *8*, 915.
(36) Pattern No. 75-0279, JCPDS (2000).
(37) Pattern No. 48-0123, JCPDS (2000).
(38) Pattern No. 42-1467, JCPDS (2000).
(39) Brinker, C. J.; Scherer, G. W. *Sol-Gel Science*: *The Physics and the Chemistry of Sol-Gel Processing*; Academic Press: New York, 1990.
(40) Pattern No. 37-0804, JCPDS (2000).

which, in turn, depend on the peculiarities of the two synthetic procedures.

Finally, thermal treatment at 900 °C for 2 h induced lanthanum cobaltite decomposition, as indicated by the appreciable intensity decrease of the corresponding diffraction peaks and the appearance of other signals in the region $25° < 2\vartheta < 32°$, ascribable to lanthanum oxides and carbonates.[19,40]

Irrespective of the preparation route, a careful inspection of $LaCoO_3$ GIXRD patterns revealed a peak shift at higher 2ϑ values compared to those reported for bulk $LaCoO_3$.[36,37] Such behavior could depend on the adopted incidence angle ($\vartheta_i = 0.5°$).[19,41,42] Under these conditions, refraction of incident X-rays at the air−solid interface has been reported to induce a peak shift at incidence angles lower than the critical angle for total external reflection.[41]

The surface and in-depth chemical compositions were investigated by XPS and XE-AES. Irrespective of the preparation procedure, analyses of the as-prepared samples revealed the absence of La-related signals on the surface, indicating a homogeneous coverage by the cobalt oxide-based overlayer. The O1s surface peak could always be fitted by three components, ascribed to lattice oxygen in a cobalt oxide-based network (BE = 530.3 eV, full width at half-maximum (fwhm) = 1.7 eV), hydroxyl species (BE = 531.7 eV, fwhm = 1.5 eV), and adsorbed water (BE = 533.0 eV, fwhm = 2.1 eV).[22,32,43]

A significant compositional evolution was observed after the annealing treatment. In the case of films obtained by SG deposition of cobalt oxide on La−O-based specimens prepared by CVD (Figure 1a) and annealed at 700 °C, 1 h, there were no F-related peaks on the surface or in the inner layers, indicating the occurrence of fluorine elimination under the adopted conditions. Conversely, F removal did not occur when only LaO_xF_y was deposited and annealed. Taken together, these phenomena suggest that the thermally induced reaction between La−O−F and Co−O phases, which yields the formation of $LaCoO_3$, was also responsible for fluorine elimination. Moreover, the surface La3d photoemission line had the typical band shape of La(III)-based oxides (Figure 3a), characterized by a double-peak structure for each spin−orbit component. These spectral features could be ascribed either to energy loss phenomena ("shake-down" satellites) induced by intense O2p → La4f charge-transfer events[34] or to strong final state mixing of electronic configurations.[31,44] The $La3d_{5/2}$ BE (834.7 and 838.1 eV) values were in agreement with the presence of $LaCoO_3$.[18,31] As concerns cobalt, the surface $Co2p_{3/2}$ BE (780.1 eV, fwhm = 3.0 eV) and the experimental $Co2p_{3/2}-Co2p_{1/2}$ energy splitting (15.2 eV) were in good agreement with the literature data for $LaCoO_3$ (Figure 3b).[10,44−46] Furthermore, the absence of

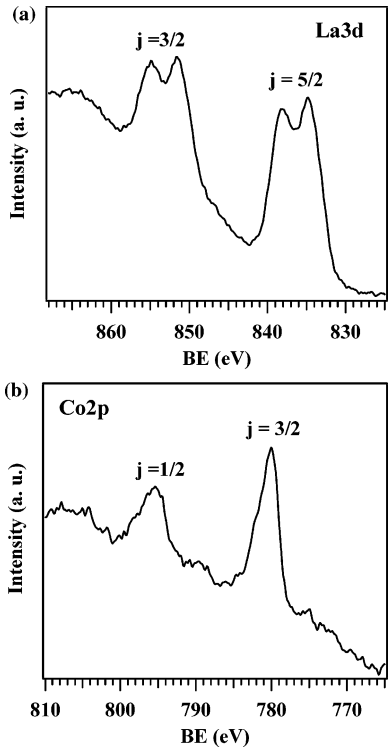

Figure 3. **(a)** La3d and **(b)** Co2p XPS surface peaks for a $LaCoO_3$ specimen obtained by SG of Co−O species on a CVD La−O-based substrate and annealing in air at 700 °C, 1 h.

appreciableshake-up satellites indicated that no Co(II) centers could be unambiguously identified.[28] The formation of pure $LaCoO_3$ in the near-surface regions was confirmed by evaluating the Auger parameter for Co (α = BE($Co2p_{3/2}$) + KE(CoLMM) = 1552.3 eV), which was very close to the literature value.[18,44] Very similar spectral features were observed for specimens obtained by CVD of cobalt oxides on $LaO_x(OA)_y$ xerogels (Figure 1b) and subsequently annealed in air at 800 °C for 3 and 5 h, in agreement with GIXRD data.

In all $LaCoO_3$ specimens, three different components contributed to the O1s band shape. The first one, at BE = 528.9 eV (fwhm = 1.5 eV), was shifted to lower BEs than those of the as-prepared samples and attributed to lattice oxygen in a lanthanum cobaltite network.[10,44] The other components, at BE = 530.5 eV (fwhm = 2.3 eV) and 532.0 eV (fwhm = 2.4 eV), were ascribed to the presence of adsorbed oxygen[10,44] and of hydroxyl species,[10,32] respectively, arising from the atmospheric exposure of the samples.

In-depth element distribution was analyzed by XPS profiles. The composition vs depth for two representative samples obtained by CVD deposition of Co−O on $LaO_x(OA)_y$ xerogels is reported in Figure 4. As regards the as-prepared specimen (Figure 4a), three different regions can be distinguished along the film thickness. In the outermost one, a predominance of Co−O-containing species can be clearly detected, in accordance with GIXRD results showing the formation of crystalline Co_3O_4. Moreover, it is worth noting that in-depth Co penetration (average Co atomic percentage ≈5%) was observed up to the substrate interface (region II),

(41) Toney, M. F.; Brennan, S. *Phys. Rev. B* **1989**, *39*, 7963.
(42) Gelfi, M.; Bontempi, E.; Roberti, R.; Armelao, L.; Depero, L. E. *Thin Solid Films* **2004**, *450*, 143.
(43) Armelao, L.; Barreca, D.; Gross, S.; Tondello, E. *Surf. Sci. Spectra* **2001**, *8*, 14.
(44) Armelao, L.; Bettinelli, M.; Bottaro, G.; Barreca, D.; Tondello, E. *Surf. Sci. Spectra* **2001**, *8*, 24.
(45) Saitoh, T.; Mizokawa, T.; Fujimori, A.; Takeda, Y.; Takano, M. *Surf. Sci. Spectra* **1999**, *6*, 302.
(46) Schenck, C. V.; Dillard, J. G.; Murray, J. W. *J. Colloid Interface Sci.* **1983**, *95*, 398.

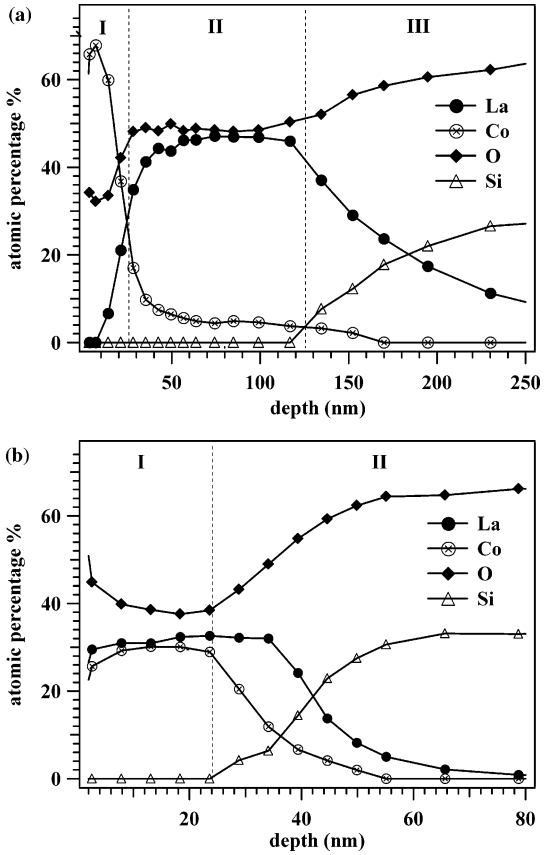

Figure 4. XPS depth profiles of two selected specimens obtained by CVD of cobalt oxides on $LaO_x(OA)_y$ xerogels: **(a)** as-prepared; **(b)** annealed in air at 800 °C, 5 h.

owing to a vapor infiltration of the Co precursor and related fragments inside the $LaO_x(OA)_y$ xerogel. This intermixing in the as-prepared sample is expected to favor the subsequent reaction between cobalt and lanthanum-containing species yielding $LaCoO_3$ under thermal treatment. In the inner region (III), an increase in Si and La atomic percentages was observed. Furthermore, a small carbon amount (≈2%) was present through the film thickness and attributed to the presence of both −OR groups, arising from the preparation procedure, and adsorbed CO_2.[34]

After annealing at 800 °C for 5 h (Figure 4b), the overall multilayer structure underwent an appreciable thickness reduction (from 170 nm, for the as-prepared sample, to ≈40 nm), which was ascribed to densification and crystallization processes induced by thermal treatment. In this case, a more uniform distribution of elements was observed, confirming an increased intermixing between La and Co phases induced by the annealing process. As a matter of fact, Co and La atomic percentages vs depth underwent appreciable changes, resulting in a La/Co ratio very close to 1 from the surface up to ≈25 nm depth (region I). Such behavior proved the formation of pure $LaCoO_3$ in the outermost sample layers. However, an underlying region (II) characterized by an excess of lanthanum with respect to cobalt indicated that the formation of lanthanum cobaltite did not regard the whole film thickness. This concentration gradient may be the result of diffusion kinetics, which probably prevented the obtainment of uniform La/Co profiles. To further clarify this phenomenon, GIXRD scans were performed on this specimen at incidence angles variable between 0.5° and 1.5°, with

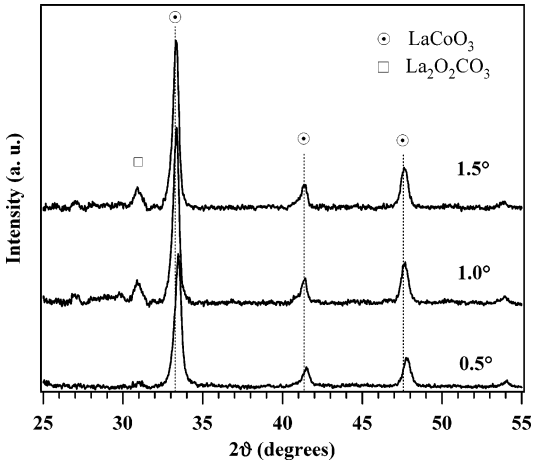

Figure 5. GIXRD scans collected at different incidence angles for a $LaCoO_3$ system obtained by CVD of cobalt oxide on a $LaO_x(OA)_y$ xerogel and annealing in air at 800 °C, 5 h. The peak positions for bulk $LaCoO_3$ [36,37] are evidenced.

the aim of investigating the eventual presence of different phases at different depths. The obtained results (Figure 5) showed that, at angles higher than 0.5°, a signal at $2\vartheta \approx 30°$ appeared along with $LaCoO_3$ reflection and was ascribed to $La_2O_2CO_3$.[40] Therefore, while $LaCoO_3$ was the only crystalline phase in the outermost sample layers, the inner ones were La-rich, as confirmed by XPS analysis (see above). This segregation of lanthanum oxycarbonate was attributed to the easy interaction of the $LaO_x(OA)_y$ xerogels with CO_2 produced in the pyrolysis of organic ligands, as observed for similar metal complexes.[47,48] Furthermore, contributions from CO_2 uptake by the outer atmosphere before the Co−O overlayer deposition might also contribute to the observed phenomenon.[49] Consequently, thermal treatment produced the crystallization of $La_2O_2CO_3$ in the inner sample layers. The presence of this phase confirmed the contribution of thermal diffusion processes in the production of a La/Co concentration gradient across the film thickness, as discussed above.

A different behavior was observed in the case of specimens obtained by SG deposition of cobalt oxide on La−O-based specimens prepared by CVD (Figure 1a) and annealed at 700 °C, 1 h. In this case, both GIXRD scans at different incidence angles and XPS depth profiling revealed the formation of pure and crystalline lanthanum cobaltite with a stoichiometric La/Co ratio throughout the film thickness. Such behavior, which once again emphasizes the different properties of specimens prepared by the two routes in Figure 1, could suggest that La−O−F films obtained by CVD have a lower reactivity with CO_2 with respect to $LaO_x(OA)_y$ xerogels, thus preventing the formation and crystallization of lanthanum oxycarbonates.

To conclude, it is worth observing from Figure 5 that GIXRD patterns collected at incidence angles higher than 0.5° restored the lanthanum cobaltite peak positions observed for the bulk material (see above).

(47) Hitchman, M. L.; Shamlian, S. H.; Condorelli, G. G.; Chabert-Rocabois, F. J. *J. Alloys Compd.* **1997**, *251*, 297.
(48) Hussein, G. A. M.; Ismail, H. M. *Powder Technol.* **1995**, *84*, 185.
(49) Nieminem, M.; Putkonen, M.; Niinistö, L. *Appl. Surf. Sci.* **2001**, *174*, 155.

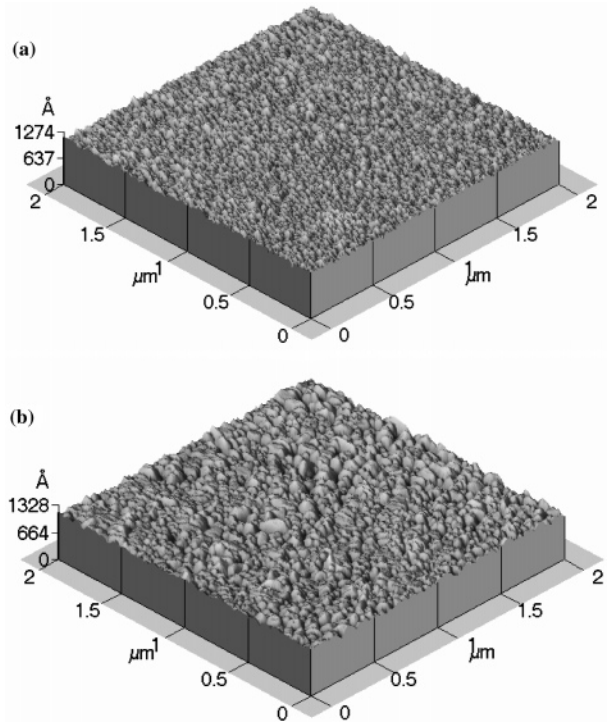

Figure 6. Representative AFM micrographs ($2 \times 2\ \mu m^2$) for two selected specimens obtained by CVD of cobalt oxides on $LaO_x(OA)_y$ xerogels: **(a)** as-prepared; **(b)** annealed in air at 800 °C, 5 h.

For all the synthesized specimens, AFM analyses revealed the presence of uniform and crack-free surface morphologies, characterized by well-interconnected globular aggregates. A very similar behavior under annealing was observed for specimens obtained by both routes in Figure 1. Representative images of samples obtained by CVD of cobalt oxides on $LaO_x(OA)_y$ xerogels (Figure 1b) are reported in Figure 6. The as-prepared specimen presented a homogeneous texture and a typical granular morphology with an average particle size of ∼40 nm. In agreement with previous results,[28] this morphology suggested a three-dimensional growth mode of cobalt oxides on $LaO_x(OA)_y$ xerogels, probably promoted by the presence of −OH groups that favor the Co precursor decomposition. After annealing at 800 °C, 5 h, which corresponded to the formation of lanthanum cobaltite (Figure 6b), an increase in the average grain size up to ≈100 nm was observed. Such behavior could be ascribed to a progressive particle agglomeration and/or coalescence induced by more severe thermal treatment. It is interesting to note that, unlike the grain size estimated by AFM measurements, the average crystallite dimensions evaluated by XRD measurements were almost unchanged by the annealing temperature. In this regard, it is worth noting that particles forming the films, whose dimensions were higher than those of nanocrystals estimated by GIXRD, were likely composed by several crystallites and/or some amorphous phase at lower annealing temperatures.

Conclusions

This work presents an innovative synthetic route to lanthanum cobaltite nanosystems based on suitable combinations of the CVD and SG routes. In particular, the approach was based on the sequential deposition of binary oxide systems (cobalt oxide-based overlayer on lanthanum oxide-based substrates) and on the optimization of the relative La/Co amounts. The deposition processes were accompanied by ex situ thermal treatments in air at temperatures between 400 and 900 °C for 1−8 h, aimed at favoring solid-state reactions between La−O and Co−O species, yielding ternary La−Co−O nanosystems. To evidence the peculiar influence of the synthesis techniques on the characteristics of the final product, both SG and CVD routes were used for the preparation of the single-phase films.

The obtained results evidenced the formation of $LaCoO_3$ nanosystems (typical crystallite size lower than 20 nm), with a system evolution depending on the particular synthetic pathway and operational parameters. In fact, such a result was achieved at temperatures of 700 °C, 1 h, when SG Co−O layers were deposited onto CVD La−O-based substrates. In this case, the CVD precursor used for lanthanum ($La(hfa)_3$·diglyme) yielded lanthanum oxyfluoride-based layers, but F-containing species could be eliminated in the thermally induced reaction with the Co−O phase. Moreover, the ternary La−Co−O phase was evenly distributed throughout the film thickness, with no Co−O and/or La−O undesired species. When the deposition techniques adopted for the two layers were inverted, a minimum annealing temperature of 800 °C was required to obtain $LaCoO_3$. In this case, GIXRD and XPS measurements revealed the segregation of a $La_2O_2CO_3$ underlayer, ascribed to the chemical affinity of lanthanum-based oxides for CO_2, which underwent crystallization under annealing. Irrespective of the preparation conditions, $LaCoO_3$ nanosystems presented a grainlike texture, with particle dimensions increasing proportionally to the annealing temperature.

The results obtained in the present work open new and intriguing perspectives concerning the role of the deposition procedure and, in particular, the deposition order of binary Co−O and La−O systems. To this aim, further experiments regarding the use of cobalt oxide as an underlayer for lanthanum cobaltite preparation will be performed in a similar fashion, to obtain a deeper insight into $LaCoO_3$ characteristics as a function of synthesis conditions. The final aim of this research project is the design and development of lanthanum cobaltite-based catalysts and sensor devices with improved functional performance.

Acknowledgment. We are grateful to Dr. C. Sada (INFM and Department of Physics, Padova University) for film thickness measurements and to Drs. P. Maritan and O. Marcon (Department of Chemistry, Padova University) for useful help in the experimental work. The work was financially supported by Research Program FIRB-MIUR−RBNE019H9K "Manipolazione molecolare per macchine nanometriche".

CM0489643